AIAA 81-4260

Optimum Tail Shapes for Bodies of Revolution

A. M. O. Smith,* T. R. Stokes Jr., † and R. S. Lee‡
McDonnell Douglas Astronautics Company, Huntington Beach, Calif.

This paper has a dual purpose: to describe a method of designing short tails for bodies of revolution that satisfy Stratford's criterion for zero shear at the wall, and to show a few shapes that have been calculated. Stratford's original two-dimensional solution, extended to axisymmetric flow, has been used to implement the procedure. The method involves simultaneous solution of the extended Stratford equation together with the necessary boundary conditions by means of an inverse potential flow program. Tails designed by this procedure are entirely at incipient separation (no skin friction); therefore the pressure recovery is the most rapid possible, making the resultant tail the shortest possible, subject to no separation. The final result is a geometry uniquely determined for freestream conditions, the transition point, and of course the basic forebody. The computer program can operate in one of two modes: 1) the forebody geometry can be maintained (except for a small region near the tail juncture) with only the tail shape determined by the method or 2) the forebody velocity distribution can be maintained up to the point of pressure recovery. The forebody geometry will then be altered for some distance upstream of the tail juncture. A number of solutions are presented for both of the above modes.

Nomenclature

A = reference area
$C_{D_{vol}}$ = drag coefficient based on (volume)$^{2/3}$
C_{D_*} = drag coefficient based on frontal area
C_p = pressure coefficient, $C_p = 1 - u^2/u_\infty^2$
$\bar{C}_p$ = Stratford type pressure coefficient $\bar{C}_p = 1 - u^2/u_0^2$
ℓ = reference length
L = length representative of the length of the body
r = radius of body at any point
R_θ = Reynolds number, $u_0 s/\nu$
s = distance along body surface, see Fig. 1
u = velocity along body outside the boundary layer
u_∞ = freestream velocity

Subscripts

0 = point at which the pressure rise starts or the body begins its main contraction, see Fig. 1
tr = transition

Introduction

THE tail of any body that moves through a fluid is an appendage that is usually added to "streamline" or to reduce the drag by permitting better pressure recovery. It is not necessarily desirable otherwise. If overall length is fixed, part of the volume of the main body must be sacrificed to provide the necessary tail length. Or, if the tail is just added to a basic body, the body becomes longer and hence is at some disadvantage from a logistics standpoint. In any case, shortening the tail will increase the prismatic coefficient and, if done properly, should reduce the drag slightly. The gains become relatively greater if there is considerable laminar flow on the forebody because tail designs properly made for this situation are even shorter. Minimum tail lengths for bodies that use polymer additives should lie between the laminar and turbulent cases.

Stratford flows[1] are limiting types of flows in the two-dimensional case. By limiting, we mean that the flows provide the most rapid rise in pressure that is theoretically possible along the body, subject to certain simplifying assumptions. One fact of interest and of great importance is that these flows have been demonstrated and found to be docile, that is they do not separate even at moderate deviations from the ideal.[2,3] Because of this verification by test, Stratford flows have technical value. Stratford's original solution applied only to two-dimensional flows. An extension to axisymmetric flow was made in Ref. 4. Subsequently, ways were seen whereby this extended criterion could be applied to the problem of a body of revolution.

Many bodies of revolution that are of practical use have a running propeller at their rear. One might suspect that, with a very short tail, the propeller would modify the flow so much that the present designs would be unduly conservative. But, that does not seem to be the case. Reference 5 is an extensive investigation of the interaction problem. On p. 43 the authors make the following statement, "As shown in [their] Figures 12a and 12b, the suction of the propeller did not change the point of boundary-layer separation on Afterbody 3 (a very blunt tail). The distance between the propeller plane and the point of separation was 1.3 propeller diameters. The propeller induced velocity at 1.3 D_p upstream of the propeller was not strong enough to alter the characteristics of the separation." In view of this statement, it seems reasonable to ignore the propeller effects. A blunt tail may complicate the propeller design problem, but in these days when the flowfield can be calculated accurately and propellers are wake adapted, no particular body modification seems necessary. So the bodies to be presented are simple bodies of revolution, faired out to a point.

In the most exact boundary-layer theory, the transverse curvature effect is accounted for. This is the effect occurring when the boundary layer is very thick compared with the radius of the body at the same station. The Stratford method makes no accounting of this effect and so may be in considerable error when applied very near a slender, pointed tail. Experimental work is needed as a guide to improve this deficiency. The work of Patel,[6] Nakayama and Patel,[7] and Geller[8] deals with this problem but trying to combine their methods with Stratford's approach is far beyond the scope of the present study.

The shapes and some properties of a number of bodies have been calculated. Many kinds of pressure distributions or shapes could be considered, but in order to avoid excessive calculations, the studies were confined to two classes of bodies: 1) those having constant velocity over much of their length—modified Reichardt bodies, and 2) those having a constant diameter over much of their length as, e.g., conventional torpedoes.

Received June 6, 1980; revision received Dec. 24, 1980.

*Consultant.
†Senior Engineer/Scientist, Aerodynamics and Hydrodynamics Department.
‡Section Chief, Aerodynamics and Hydrodynamics Department.

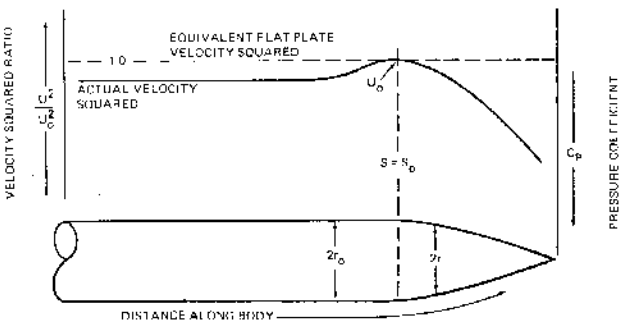

Fig. 1 Flow situation being analyzed.

As will be seen, the tail shapes that were found are quite short and are of a reflex type. D. M. Nelson[9] did work on this same tail fairing problem and arrived at a similar tail design which was confirmed to be very good by wind-tunnel tests. Nelson's approach was not as systematic as the present one and he worked out only one case. But, as far as we know, his work is the only one that is parallel to the present study. The present report is a presentation of the theoretically shortest tails for a variety of cases. Furthermore, in the case of Reichardt-type bodies, the tail and rest of the body shape are all integrated together, that is, the tail is not just an appendage on a basic Reichardt body.

Theory

The Stratford Equation and Its Use

The general kind of flow being analyzed is illustrated in Fig. 1. A flow begins to retard at some point $s=s_0$. In the vicinity of this same point the body begins to converge significantly from some initial radius r_0. At the start of the pressure recovery, the boundary layer has a momentum thickness θ_0 and an edge velocity u_0. In the analysis the notion of an equivalent flat plate was introduced by Stratford. It is of such a length s_0 with velocity u_0 as to generate the same momentum thickness θ_0 as the real body. Pressures are referenced to the velocity u_0 at s_0, not to u_∞. In particular, the pressure coefficient is defined as:

$$\bar{C}_p = 1 - u^2/u_0^2 \tag{1}$$

After this introduction to the notation and flow situation, we can write the extended Stratford formula[4]:

$$\bar{C}_p [s(r_0/r)^i (\mathrm{d}\bar{C}_p/\mathrm{d}s)]^{1/2} (10^{-6}R_0)^{-1/10} = 0.50,\ \bar{C}_p \leq 4/7 \tag{2}$$

where R_0 is a Reynolds number defined as $u_0 s/\nu$. Separation is said to occur if the left-hand side of Eq. (2) exceeds 0.50.

Stratford's equation is normally used by evaluating the left-hand side for a given body shape to learn where it exceeds 0.50. But it really is a differential equation and, if the constant is used as 0.50, it provides a solution for $\bar{C}_p(s,r)$ to produce a flow that is continuously at a condition of incipient separation. In the two-dimensional case, $i=0$, Eq. (2) can be integrated once and for all, with s_0 and R_0 as parameters. The corresponding body shape can then be found by using an inverse potential flow method. In fact that has been done in Refs. 1-3 and the flows have been tested as mentioned before, with good results.

In the axially symmetric case, $i=1$, since the body shape $r(s)$ is not known a priori, Eq. (2) can no longer be solved alone. Rather, the unknowns $\bar{C}_p(s)$ and $r(s)$ must be solved simultaneously from Eq. (2) and the potential flow equations. To this end, an iterative method has been found successful:

1) Assume an overall shape that meets certain design requirements (e.g., forebody velocity, forebody shape, L/D, etc.). The tail shape is part of the guess but will be allowed to geometrically float.

2) Use a conventional potential flow method to find $C_p(s)$, u_0, and then $\bar{C}_p(s)$.

3) Integrate Eq. (2) to find a new $\bar{C}_p(s)$ over the designated tail portion only.

4) By using an inverse method such as that of James[10] or Bristow[11] and the $C_p(s)$ from step 3, find a new $r(s)$. The forebody C_p is not altered.

5) Repeat steps 3 and 4 until convergence is achieved.

Peripheral Aspects

In potential flow it is well known that for semi-infinite cones, the velocity along the cone varies as d^m where d is the slant distance from the apex.[12] Then near the tail apex, using Eq. (1), we can write

$$\bar{C}_p = 1 - \frac{u^2}{u_0^2} = 1 - \frac{c^2 |s-a|^{2m}}{u_0^2} \tag{3}$$

Here the apex is located at $s=a$ and c is a constant for the flow. It follows that

$$\frac{\mathrm{d}\bar{C}_p}{\mathrm{d}s} = -\frac{2mc^2 |s-a|^{2m-1}}{u_0^2} \tag{4}$$

Also, for a cone we can write

$$r = b|s-a| \tag{5}$$

where b is another constant. In Eq. (2), at the tail ($s=a$) s is a number whose order is the length of the model and r_0 is the initial radius. Also being near the apex, $\bar{C}_p$ is near unity, see Eq. (3). R_0 is large, being a Reynolds number. Then it is sufficient in studying the behavior of Eq. (2) at the apex to consider $(1/r)\mathrm{d}\bar{C}_p/\mathrm{d}s$, which from Eqs. (4) and (5) becomes

$$\frac{1}{r}\frac{\mathrm{d}\bar{C}_p}{\mathrm{d}s} = -\frac{2mc^2}{u_0^2 b} |s-a|^{2m-2} \tag{6}$$

This quantity approaches infinity as $s \to a$ if $m<1$. The value $m=1$ corresponds to a blunt tail so any tail that is pointed will have a singularity. Therefore it is seen that Eq. (2) is singular at the very end of a conical tail in inviscid flow. In the present analysis, since the potential flow problem is solved by a finite-element method, the flow at the very apex is never calculated and thus the singularity is avoided. Of course, due to the boundary layer such a singularity would not exist in any real flow.

Having made these statements about behavior of the flow at the end of the tail, that is, at the end of the Stratford pressure recovery, let us consider its behavior at the beginning. The recovery begins at the point s_0. Introduce the variable s' as a measure of distance from this point. Then Eq. (2) can be rewritten as

$$\bar{C}_p^2 \mathrm{d}\bar{C}_p = 0.25(r/r_0)(10^{-6}R_0)^{1/5} \mathrm{d}s'/(s_0+s') \tag{7}$$

R_0 can be written as $(u_0/\nu)(s_0+s')$.

Just aft of s_0 where s' is very small, $r_0/r \approx 1.0$, $R_0 \approx (u_0/\nu)s_0$, and $\bar{C}_p \approx 0$. Then Eq. (7) can be integrated to give

$$\bar{C}_p^3 = 0.75(10^{-6}u_0/\nu)^{1/5} s'/s_0^{4/5} \tag{8}$$

or

$$\bar{C}_p = 0.91(10^{-6}u_0/\nu)^{1/15} (s')^{1/3}/s_0^{4/15} \tag{9a}$$

Of course Eq. (9a) can be written in numerous ways but this form perhaps best reveals the nature of Stratford flows at the very beginning of the pressure recovery.

Equation (9a) points out several facts. First and most important is that $\bar{C}_p$ begins increasing as $(s')^{1/3}$ and at the very start the increase has an infinite slope. This result which is

true for both two-dimensional and axisymmetric flows is surprising and quite interesting. It shows that if a demanded pressure rise is quite small it can be extremely rapid. Tests seem to bear out this observation.

The other facts indicated by Eq. (9a) are that the multiplier for $(s')^{1/5}$ is an extremely weak function of the unit Reynolds number and varies inversely as the flat-plate equivalent approach flow s_θ to a weak power. Thus Eq. (9a) is a weak function of s_θ except in the case of small s_θ, which may occur with laminar flow. An alternate form of Eq. (9a) is

$$\bar{C}_p = 0.91(10^{-6}R_\theta)^{1/15}(s'/s_\theta)^{1/5} \tag{9b}$$

Even though the r/r_θ term has been used as unity Eq. (9b) shows another interesting fact. $\bar{C}_p$ is a function of s'/s_θ. Then if s_θ is large, for a given pressure rise, s' must be large. If s_θ is very small, then s' can be very small. In other words, Eq. (9b) shows that the minimum required tail length is proportional to $s_\theta^{-1/5}$.

Determination of s_θ

In order to use Stratford's formula the distance s_θ must be determined. It is the length of the equivalent flat plate at velocity u_θ that generates the same thickness θ_θ as on the body that is being analyzed. A suitable formula for a general body of revolution is a modification of Truckenbrodt's equation.[13] When written for the point s_θ it is

$$\left(\frac{\theta}{\ell}\right)_{s_\theta/\ell} = \left\{\left[\frac{\theta_{tr}}{\ell}\left(\frac{u_{tr}}{u_\infty}\right)^3\frac{r_{tr}}{\ell}\right]^{7/6} + \frac{0.17775}{(\log_{10}R_L)^{3.010}} \times \int_{s_{tr}/\ell}^{s_\theta/\ell}\left(\frac{u}{u_\infty}\right)^{3.33}\left(\frac{r}{\ell}\right)^{7/6}\frac{ds}{\ell}\right\}^{6/7} \Big/ \left[(u/u_\infty)_{s_\theta}^3 (r/\ell)_{s_\theta}\right] \tag{10}$$

In Eq. (10) the first term is a measure of the laminar boundary layer at its transition point. Using the Rott-Crabtree formula[13] it can be written

$$\left(\frac{r}{\ell}\frac{\theta}{\ell}\right)_{tr}^2 = \frac{0.470\nu}{(u/u_\infty)_{tr}^6}\int_0^{(s/\ell)_{tr}}\left(\frac{r}{\ell}\right)^2\left(\frac{u}{u_\infty}\right)^5 \mathrm{d}\frac{s}{\ell} \tag{11}$$

The integral term in Eq. (10) accounts for the growth of the turbulent momentum thickness. The factor multiplying it is different from Truckenbrodt's. The factor comes from Schlichting's formula $c_f = 0.455/(\log_{10}R_L)^{2.58}$ which is more accurate over the entire Reynolds number range.[13] The term R_L is a Reynolds number that is representative of the length of the body. It is usually used as $R_L = u_\infty L/\nu$ but other values could be used in place of u_∞ and L. The term ℓ is any reference length. It could be maximum radius, body length L, etc.

To get the equivalent length of the flat plate that generates the same momentum thickness θ_θ at a velocity u_θ, use is made of the 1/7 power law velocity profile in obtaining $\theta = 0.036(u_\infty x/\nu)^{-1/5}$. This is an approximation consistent with our present boundary-layer model. When adapted to our problem and solved for s_θ we have

$$(s_\theta/\ell)_{eq} = (\theta/\ell/0.036)_{s_\theta/\ell}^{5/4}(u_\theta\ell/\nu)^{1/4} \tag{12}$$

Substitution of Eq. (10) into Eq. (12) yields the equivalent value of s_θ/ℓ.

Drag

Because Eq. (10) had to be evaluated it was quite simple to go one step further and calculate drag coefficients by means of the Squire-Young type formula, that is[14]

$$C_D = (4\pi r\theta/A)(u/u_\infty)^{(H+5)/2} \tag{13}$$

By a slight rearrangement Eq. (10) computes $r\theta$ directly. If total drag is the item of interest then all quantities in Eq. (13) are evaluated at the very tail. Because the tail flow is of an incipient separation type it is logical to assume that the shape factor $H = 2.0$. Then the u/u_∞ term in Eqs. (10) and (13) very nearly cancel each other and a final equation for these types of bodies can be written

$$C_D = \frac{4\pi\ell^2(u/u_\infty)_{tail}^{1/2}}{A}\left\{\left[\left(\frac{\theta}{\ell}\right)_{tr}\left(\frac{u}{u_\infty}\right)_{tr}^3\left(\frac{r}{\ell}\right)_{tr}\right]^{7/6} + \frac{0.17775}{(\log_{10}R_L)^{3.010}}\int_{s_{tr}/\ell}^{s_{max}/\ell}\left(\frac{u}{u_\infty}\right)^{3.33}\left(\frac{r}{\ell}\right)^{7/6}\frac{ds}{\ell}\right\}^{6/7} \tag{14}$$

This formula has been used to compute drag coefficients for the bodies. Because Truckenbrodt's formula is for thin boundary layers, but boundary layers at the tail are thick, its application may be questioned. However, Hess[17] has shown that it is within 1-2% of the most accurate solutions. In their study they assumed $(u/u_\infty)_{tail}^{1/2}$ in Eq. (14) to be equal to unity, which it very nearly is.

Some Comments on Implementation If the Bristow Method Is Used

Equation (2) cannot be integrated unless $r_0/r(s)$ is given or assumed. For the initial trial on the constant diameter bodies it was found that the form

$$r(x)/r_0 = [1-(x/L)^{1.5}]/[1+(x/L)^{1.5}] \tag{15}$$

was satisfactory for starting. With $r(x)/r_0$ given, as well as the other quantities obtained from boundary conditions, Eq. (2) could be integrated. Once it was integrated subject to forebody conditions, an entire pressure distribution was available. This then was supplied to Bristow's inverse method and the body found. The new body would have a tail different from that given by Eq. (15) and the cycle could be repeated until convergence was obtained. For the Reichardt-type bodies the initial tail shape was just the blunt tail of a classical Reichardt body.

Two cases were studied: 1) the forebody had constant diameter and 2) the forebody had constant velocity. For the first case, after a cycle through Bristow's inverse method the body would not quite be of constant diameter. It was corrected to the proper shape, pressure distribution recalculated for purposes of input to the inverse program, and together with results from Eq. (2) a new complete velocity distribution could now be used in Bristow's program. The cycle was repeated until the entire body problem converged. For case 2 the problem was somewhat simpler because forward velocities were specified in the first place.

However, the calculations involved difficulties. Selection of the point of departure was a problem if a given fineness ratio was desired because the length of the tail would not be known a priori. But a worse problem was finding the proper tail length. If the chosen tail length is too short for the desired pressure distribution, the tail will converge for a while and then flare out like a rocket nozzle. If too long, the shape will touch the axis and then oscillate. But the worst problem occurred if the guess for length was not sufficiently close. Then iterations were in total disarray and one could not tell whether the tail was too long or too short. Only if the guess was close could one see which way to go to improve the answers. Hence, the method can hardly be called a straightforward algorithm. However, a number of results were obtained.

Experience has shown that it would be virtually impossible to obtain the desired shapes by cut and try using only a direct method. The question may arise as to whether or not an iterative technique, using a direct potential flow solution, will work. It is certainly rational to conjecture an iteration of the form: 1) Guess $r(s)$, 2) obtain $C_p[r(s)]$ from a direct solution, 3) solve Eq. (2) for $r(s)$, and 4) repeat steps 2 and 3 until convergence is achieved.

Table 1 Computation schedule and pertinent output parameters

Case No.	Configuration	Re_L	Forebody state	θ_0/R	s_0/R	s_0/L	C_{D_π}	$C_{D_{vol}}$	Tail length, TL/R	$\frac{u_0/s_\theta}{\nu}\times 10^{-6}$	$C_{p_{min}}$
1	CD8	10^7	Turb.	0.0170	11.59	0.726	0.1095	0.0241	3.10	8.847	−0.492
2	CD8	10^7	Lam.	0.00120	0.4485	0.28	0.0150	0.0033	1.25	0.438	−1.437
3	R8	10^7	Turb.	0.0358	28.11	1.75	0.0761	0.0227	1.77	18.10	−0.06
4	R8	10^7	Lam.	0.00583	2.91	0.182	0.0104	0.0031	1.02	1.88	−0.07
5	R8	10^6	Turb.	0.0518	25.13	1.57	0.1152	0.0341	2.02	1.62	−0.06
6	R8	10^8	Turb.	0.0262	33.89	2.12	0.0532	0.0159	1.58	218.2	−0.06
7	CD4	10^6	Lam.	0.00297	0.9062	0.113	0.0317	0.0112	2.0	0.159	−0.98
8	R4	10^6	Lam.	0.00643	2.24	0.281	0.0209	0.0098	1.50	0.309	−0.17
9	HEMI	10^6	Turb.	0.00087	0.361	0.361	0.0274	0.0390	1.2	0.744	−3.26

It is well known from numerical analysis that any iteration of the form

$$x_{i+1}=f(x_i)$$

will converge if and only if $|df/dx|<1$ near the solution and will diverge if $|df/dx|>1$. The iteration reported herein is analogous in form to the above simple iteration. Experience has shown that C_p is very sensitive to r and using a direct potential flow solution in the iteration will lead to divergence. Conversely, r is a weak function of C_p and rapid convergence can be obtained by using an inverse potential flow solution in the iteration. Our experience has confirmed the latter case.

Results

The calculational method has been used to find several body and tail shapes. Although the tail is generally envisioned as an appendage to some forebody, it will slightly alter forebody pressures through its upstream influence. In addition, because this particular problem is solved with an inverse potential flow procedure, the entire forebody shape is slightly altered by the addition of a tail. Also, because of the nature of the extended Stratford equation, the forebody shape and its boundary-layer characteristics have a strong influence on the final tail shape; that is, the tail design is not a problem separable from the forebody design.

The two families that were analyzed can be loosely categorized as follows:

1) A prescribed forebody shape with the tail geometry being defined by the Stratford recovery region.

2) A prescribed velocity distribution up to the point of the Stratford recovery.

To be still more specific, these two families were further narrowed down to two types. For the first family, a hemisphere-cylinder was chosen, as it is rather representative of conventional torpedo designs. Various cylinder lengths are presented including a zero-length cylinder (i.e., a hemisphere-tail). For the second family, a constant-velocity solution from the Reichardt class of bodies was prescribed. Again, results are presented for various slenderness ratios.

Table 1 presents a summary of all cases computed under the guidelines established above. Each particular case in Table 1 is identified by a configuration code of the form CDX or RX. The CDX code signifies a constant-diameter body (hemisphere-cylinder) with X representing the length-to-diameter ratio of the basic forebody. One exception to this convention is the CD1 body (no cylinder section) which is simply called HEMI for hemisphere only. The RX nomenclature is used for the constant-velocity shape which comes from the Reichardt class of bodies. Again, X represents the slenderness ratio of the basic Reichardt body. Also presented in Table 1 are the pertinent flow conditions, such as the freestream Reynolds number based on body length and the state of the boundary layer on the forebody (laminar or turbulent), and the pertinent results.

As was pointed out in the preceding section, the final tail length is not known a priori as it is a function of Reynolds number, boundary-layer state, and forebody geometry.

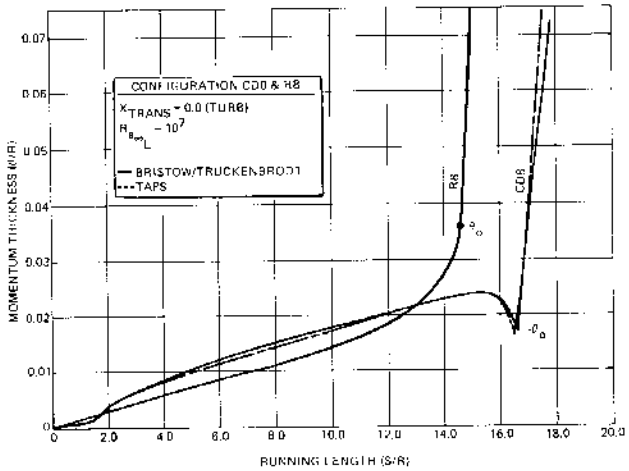

Fig. 2 Predictions of momentum thickness distribution for CD8 and R8 bodies.

Hence, for purposes of being consistent, the length parameter is a length referenced to some nonvarying geometrical dimension of the body. For the CD class of bodies, the reference length was chosen as the distance from the nose to the end of the cylinder. In the case of the HEMI body, this reduces to the hemisphere radius. For the R class of bodies, the reference length is that of the unmodified Reichardt geometry (fore and aft symmetry).

Since the boundary-layer momentum thickness plays such an important role in the determination of the final tail shape, a test case was prepared from case 1 and checked using the more exact Cebeci-Smith boundary-layer method[15] as implemented in the TAPS computer code.[16] The results of this test case are presented in Fig. 2. As can be seen, the momentum thicknesses as computed by the two methods are in remarkably good agreement. The most crucial value for θ is θ_0 which determines s_0 by Eq. (12). The θ_0 point in Fig. 2 occurs exactly at the minimum just aft of $s/r=16$. Here, the two computer programs are in such good agreement that the result seems almost fortuitous. Judging from the overall trends in the two curves, the Bristow/Truckenbrodt method appears to be more than adequate.

For comparative purposes, a similar momentum thickness distribution for the R8 body is also presented in Fig. 2. The manner of boundary-layer growth as compared to the constant-diameter CD8 body is quite different. As a consequence of the conservation of mass in axisymmetric flows [$r(s)$ effect], the boundary-layer growth on Reichardt shapes is inhibited everywhere forward of the point of maximum diameter. Aft of this point, the thickness begins to increase more rapidly, such that by the time the Stratford recovery begins, the boundary layer is quite thick relative to a body of constant diameter. In contrast, the boundary-layer development on constant-diameter bodies has a more or less flat-plate behavior until the flow begins to accelerate near the tail juncture. From Eq. (10) it can be seen that locally (for small variations

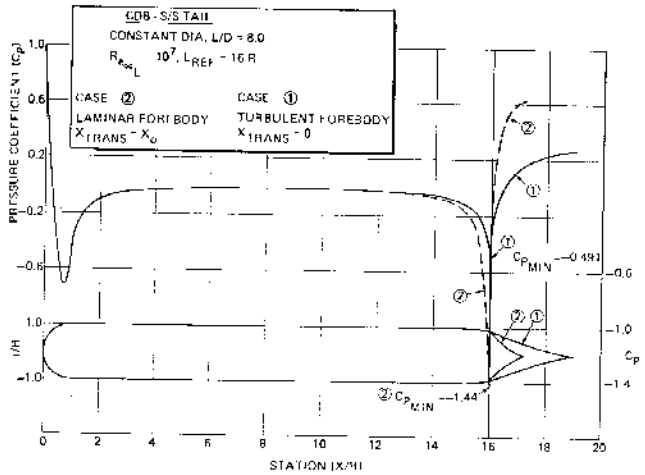

Fig. 3 Tail designs for laminar and turbulent flows over a hemisphere-cylinder forebody ($L/D = 8$).

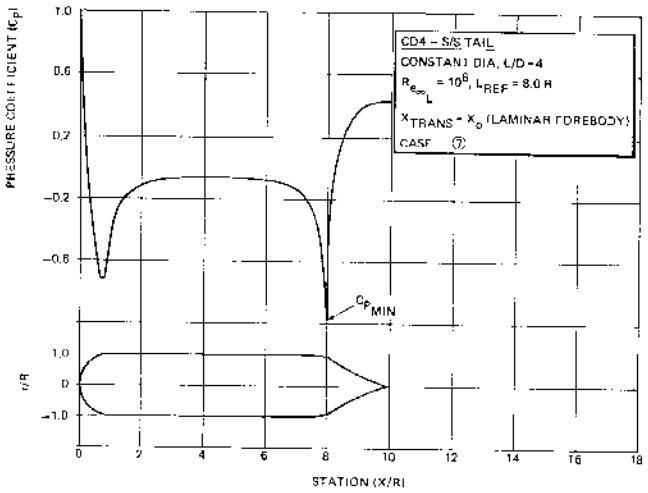

Fig. 4 Tail design for a hemisphere-cylinder forebody ($L/D = 4$).

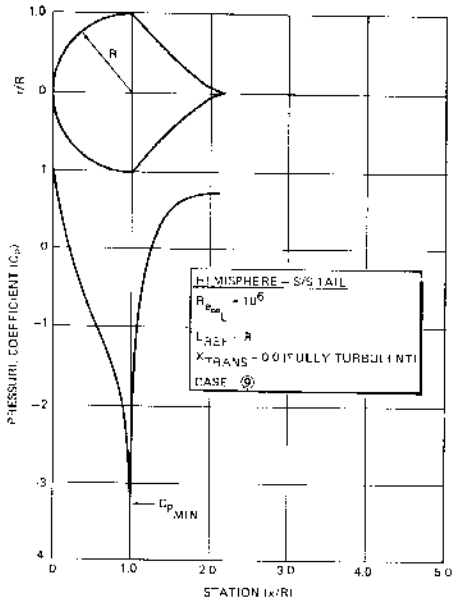

Fig. 5 Tail design for a hemisphere forebody.

in s), θ varies inversely as $(u_e/u_\infty)^3$. Since (u_e/u_∞) is not constrained in the constant-diameter solutions, θ will minimize at the tail juncture where, by definition, θ_0 and s_0 are determined.

This localized thinning effect has a very interesting feedback influence on the tail length for the constant-diameter bodies. The reduction in θ_0 promotes smaller values of s_0 as seen by Eq. (12). Due to the nature of the extended Stratford equation as discussed previously, smaller s_0 values tend to drive the tail length still shorter. The shorter tail lengths in turn produce still higher corner velocities and smaller values of θ_0. Thus, we have the pleasantly surprising result that the combined effects of the extended Stratford equation, the potential flow relations and boundary-layer equations have a built-in "forcing function" that results in extremely short tails. This forcing function is even more pronounced in the case where the forebody is laminar since the momentum thickness is much smaller.

Two converged solutions that graphically indicate these effects are depicted in Fig. 3. The two solutions are from cases 1 and 2 which are for the CD8 body at a Reynolds number of 10^7. The only difference is that case 1 is for a fully turbulent forebody while case 2 is laminar up to the jail juncture. As can be seen, the boattails for both cases are quite short and the pressure recovery exhibits a typical Stratford behavior. In taking a cursory look at the laminar flow body, the tail appears so short that it intuitively invites disbelief. Its shortness is directly attributable to the combined effects of small θ_0, the resultant small s_0, and the deep pressure spike leading into the pressure recovery. All of these parameters are presented in Table 1 for a case-to-case comparison.

To validate further the reported procedure of finding Stratford tail shapes, two other cases of fixed forebody geometries are presented in Figs. 4 and 5. Figure 4 is a constant-diameter, $L/D = 4$ body. In this example, the forebody is laminar and the Reynolds number is 10^6. For it, the tail length came out somewhat longer (in terms of maximum body radius) than the CD8 body. This result is directly attributable to the reduced Reynolds number of the flow. Referring to Table 1, the computed value for s_0 on the CD4 body at $R_{e_L} = 10^6$ is 0.906 R, whereas on the longer CD8 body at $R_{e_L} = 10^7$, s_0 is 0.448 R. The larger value for s_0, when coupled with the extended Stratford equation, requires a longer tail. The laminar forebody is unrealistic because laminar separation and transition will surely occur at the rear of the hemisphere.

Figure 5 is a hemisphere followed immediately by a Stratford recovery tail. This case was computed at a relatively low Reynolds number, 10^6, with a fully turbulent forebody. This results in probably the *longest* tail necessary. That is, higher Reynolds numbers and/or some forebody laminarization could lead to a still shorter tail using the extended Stratford guidelines. Even for this case, however, the true L/D of this body is only 1.1. Furthermore, the solution was obtained with relative ease, which indicates that still blunter forebodies (e.g., oblate spheroids) could be closed using the Stratford recovery method.

Thus far, all the cases discussed are of the "prescribed forebody" type. As was evident in the figures, this approach will almost invariably lead to deep, negative pressure spikes at the tail juncture. In high-speed underwater regimes, such low-pressure areas may be intolerable from a cavitation standpoint. To alleviate this problem, the present method allows for constraining the forebody velocity up to the beginning of the pressure rise. One of the classical high-speed underwater shapes is the Reichardt body. For reasonable fineness ratios this geometry has a surface velocity that is nearly constant and nowhere exceeds the freestream velocity by more than 5-10% or so. Thus, it was felt that Reichardt shapes would be good candidate bodies for applying the Stratford recovery method for tail design.

Figure 6 presents the results of applying the present method to Reichardt bodies with an initial L/D of 8. Two cases (3 and 4 in Table 1) are included in the figure. The only initial conditions that are different is that case 3 has a fully turbulent forebody while case 4 is laminar up to the start of the pressure rise. As is evident in the figure, the present method of coupling the extended Stratford equation with an inverse

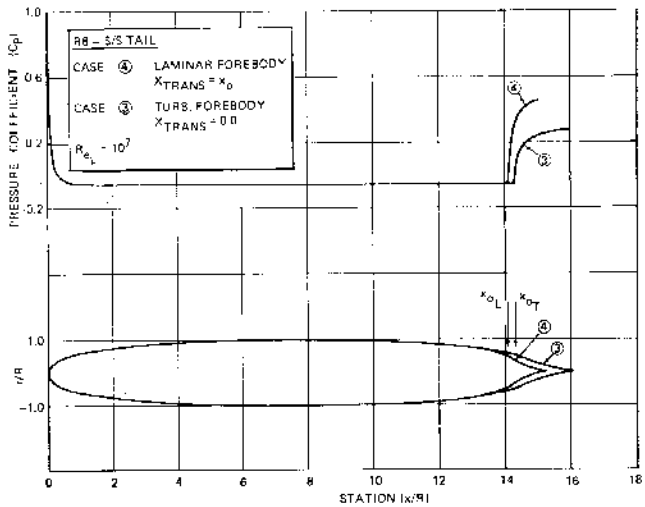

Fig. 6 Tail designs for a Reichardt body ($L/D = 8$).

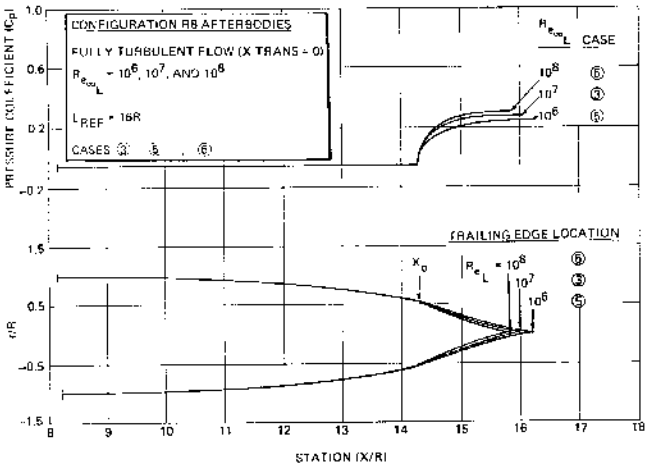

Fig. 7 Effect of Reynolds number on tail design for fully turbulent flows.

potential flow solution allows for maintaining the constant velocity up to the point of the Stratford recovery. When applied in this mode, however, the geometry of the forebody will be noticeably modified for several diameters forward of the point where the pressure rise begins, because of the elliptic nature of the potential flow equation.

Also evident in Fig. 6 is that the start of the pressure rise does not occur at exactly the same station for the two cases. The reason is twofold: first, where the pressure recovery starts in a constant-velocity region is an arbitrary choice and, second, the required length of the tail can dictate the start of the pressure rise for reasons of computational ease.

Some of the important output parameters from the two cases are summarized in Table 1. For example, the computed values of s_0 for the R8 configurations (cases 3 and 4) are considerably larger than their counterparts on the CD8 bodies (cases 1 and 2). As discussed earlier, this is due to the extensive thickening of the boundary layer on the aft end of Reichardt shapes. In addition, the lack of high velocities that are permitted in cases of fixed forebody geometries is a contributor. These effects are reflected in the tabulated values of $\theta_0, C_{p\min}$, and $u_0 s_0/\nu$.

In order to assess the impact of Reynolds number on tail design, the Reynolds number of 10^7 in case 3 is complemented by cases 5 and 6 which are at Reynolds numbers of 10^6 and 10^8, respectively. The afterbody shapes and pressure distributions from these cases are presented in Fig. 7. The significant conclusion to be made from this example is that tail shapes in

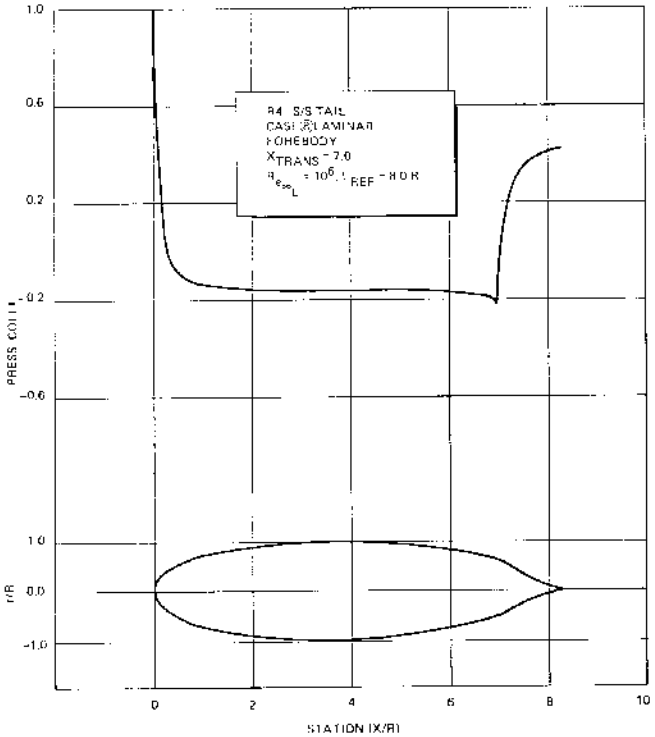

Fig. 8 Tail design for a Reichardt body ($L/D = 4$).

fully turbulent flows are not appreciably affected over a wide range of Reynolds numbers. Thus, a tail that is optimally designed for the lower end of the anticipated Reynolds number range will be nearly optimum with increasing Reynolds number. Alternately, if the design process has some built-in conservatism, e.g., a reduced value of the constant in Eq. (2), then Reynolds number should not play an important role in tail design. Of course, all of these statements are based on the assumption that the forebody will remain turbulent. If the forebody should become laminar, or partially laminar, the tail will simply be off-design, but conservative, and will not have separated flow.

The last geometry to be reported is from case 8 (Fig. 8). This is the R4 configuration at a Reynolds number of 10^6 with a laminar forebody. Although this particular case was primarily included as a further substantiation of the reported method, it does have some interesting attributes. For example, C_D based on the two-thirds power of the volume is only 0.0098. Although some of the longer shapes have smaller C_D values, it is because laminar flow was assumed to exist at a Reynolds number of 10^7. Those cases were included only to show the potential if some sort of laminar flow control were used. Hence, for practical application, the R4 laminar flow body is a good candidate configuration where drag is of primary concern. In fact, the tail optimization procedure could be exercised for a variety of forebody shapes in an attempt to minimize overall drag. Furthermore, the method is not restricted to an underwater regime and the concept is equally applicable to two-dimensional flows.

In a paper by Hess[17] there are several conclusions for fully turbulent flow which are quoted here verbatim.

"1) A shape having the lowest drag at one Reynolds number has the lowest drag at all Reynolds numbers.

"2) Shapes with fineness ratios in the range of 3 to 4 have the lowest drag coefficients based on the two-thirds power of the volume.

"3) Drag coefficient is insensitive to shape and no shape has been found with significantly lower drag than a boattailed prolate spheroid. A more accurate drag calculation might modify these conclusions slightly, but would probably not drastically revise them."

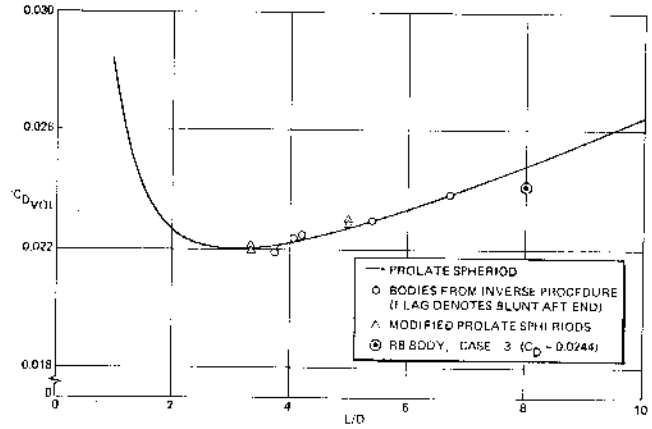

Fig. 9 Calculated drag coefficients vs fineness ratio for constant-pressure bodies at Reynolds number of 10^6.

In all, some 50 bodies were investigated by Hess and some of these bodies were of the constant-velocity type described herein. Moreover, the boattails were merely streamlined to prevent separation and no optimization procedures were employed. Figure 9, which is taken directly from his paper, is one example from which their conclusions were based. This figure is chosen for inclusion here since it portrays the drag behavior of modified Reichardt shapes (constant velocity shapes with a streamlined tail). One data point from our results is suitable for inclusion on this figure and has been added. It is for the R8 body of case 3 and indicates that a slight drag reduction is obtainable through proper tail optimizing procedures. Tails on all the other bodies in the figure were conventional. This one, being mostly concave, may indeed demonstrate the drag reduction that has been calculated. The drag values in Table 1 were all calculated by Eq. (14). The R8 point in Fig. 9 let $(u/u_\infty)^{\frac{1}{5}}_{\text{tail}}$ in Eq. (14) be equal to unity to maintain internal consistency.

The body coordinates are available upon request.

Conclusion

While some extremely short tails have been indicated, for conventional turbulent boundary layers the calculated tail is not shorter than already developed. In Ref. 9 a conventional tail of a torpedo is indicated as being about 2.8 diameters long. Nelson's special development in Ref. 9 was 1.7 diameters long. It should be noted that both of these tails were truncated when the diameter decreased to about 16% of the beginning diameter. The most comparable tail in this report is that for the CD8 in Fig. 3. Its fineness ratio is about 2.0. If it could safely be truncated as were those of Ref. 9 its fineness ratio would be about 1.75 or nearly the same as Nelson's. In conclusion, it can be said that a major contribution of this paper is to provide a rational and systematic approach for designing tails that have substantially minimum length. If laminar flow can ever be counted on, some extremely short tails are indicated. A second contribution is to point out the relation of the length of the tail to the boundary layer that approaches the tail.

Acknowledgment

This work was supported by the General Hydromechanics Research Program of the David W. Taylor Naval Ship Research and Development Center, under Contract N00014-77-C-0672 administered by Stuart F. Crump.

References

[1] Stratford, B.S., "The Prediction of Separation of the Turbulent Boundary Layer," *Journal of Fluid Mechanics*, Vol. 5, No. 1, 1959, pp. 1-16.

[2] Liebeck, R. H., "A Class of Airfoils Designed for High Lift in Incompressible Flow," *Journal of Aircraft*, Vol. 10, Oct. 1973, pp. 610-617.

[3] Liebeck, R. H., "Wind Tunnel Tests of Two Airfoils Designed for High Lift Without Separation in Incompressible Flow," McDonnell Douglas Rept. MDC J5667-01, 1972.

[4] Smith, A.M.O., "Stratford's Turbulent Separation Criterion for Axially-Symmetric Flows," *Journal of Applied Mathematics and Physics (ZAMP)*, Vol. 28, 1977, pp. 929-939.

[5] Huang, T. T., Wang, H. T., Santelli, N., and Groves, N. C., "Propeller/Stern/Boundary-Layer Interaction on Axisymmetric Bodies: Theory and Experiment," NSRDC Rept. 76-0113, 1976.

[6] Patel, V. C., "A Simple Integral Method for the Calculation of Thick Axisymmetric-Turbulent Boundary Layers," *Aeronautical Quarterly*, Vol. 25, Pt. I, 1974, pp. 47-58.

[7] Nakayama, A. and Patel, V. C., "Calculation of the Viscous Resistance of Bodies of Revolution," *Journal of Hydronautics*, Vol. 8, Oct.-Dec. 1974, pp. 154-162.

[8] Geller, E. W., "Calculation of Flow in the Tail Region of a Body of Revolution," *Journal of Hydronautics*, Vol. 13, Oct.-Dec. 1979, pp. 127-129.

[9] Nelson, D. M., "Development of a Blunt Afterbody Configuration for the RETORC Torpedo," Naval Undersea Warfare Center Rep. NUWC TP-15, 1968.

[10] James, R. M., "A General Analytical Method for Axisymmetric Incompressible Potential Flow About Bodies of Revolution," *Computer Methods in Applied Mechanics and Engineering*, Vol. 12, 1977, pp. 47-67.

[11] Bristow, D. R., "A Solution to the Inverse Problem for Incompressible Axisymmetric Potential Flow," AIAA Paper 74-520, 1974.

[12] Hess, J. L. and Faulkner, S., "Accurate Values of the Exponent Governing Potential Flow About Semi-Infinite Cones," *AIAA Journal*, Vol. 3, April 1965, p. 767.

[13] Schlichting, H., *Boundary Layer Theory*, McGraw-Hill Book Co., New York, 1968, Chap. XXII.

[14] Young, A. D., "The Calculation of Total and Skin Friction Drags of Bodies of Revolution at Zero Incidence," ARC R&M 1874, 1939.

[15] Cebeci, T. and Smith, A. M. O., *Analysis of Turbulent Boundary Layers*, Academic Press, New York, 1974, sec. 7.3.

[16] Gentry, A. E., "The Transition Analysis Program System," McDonnell Douglas Rept. MDC J7255, 1976.

[17] Hess, J. L., "On the Problem of Shaping an Axisymmetric Body to Obtain Low Drag at Large Reynolds Number," *Journal of Ship Research*, Vol. 20, No. 1, 1976, pp. 51-60.